

Blind Local Noise Estimation for Medical Images Reconstructed from Rapid Acquisition

Xunyu Pan, Xing Zhang and Siwei Lyu

Computer Science Department, University at Albany, SUNY
Albany, New York 12222, USA

ABSTRACT

Developments in rapid acquisition techniques and reconstruction algorithms, such as sensitivity encoding (SENSE) for MR images and fan-beam filtered backprojection (fFBP) for CT images, have seen widely applications in medical imaging in recent years. Nevertheless, such techniques introduce spatially varying noise levels in the reconstructed medical images that may degrade the image quality and hinder subsequent diagnostic inspection. Though this may be alleviated with multiple scanning images or the sensitivity profiles of imaging device, these pieces of information are typically unavailable in clinical practice. In this work, we describe a novel local noise level estimation technique based on the near constancy of kurtosis of medical image in band-pass filtered domain. This technique can effectively estimate noise levels in the pixel domain and recover the noise map for reconstructed medical images with nonuniform noise distribution. The advantage of this method is that it requires no prior knowledge of the imaging devices and can be implemented when only one single medical image is available. We report experiments that demonstrate the effectiveness of the proposed method in estimating the local noise levels for medical images quantitatively and qualitatively, and compare its estimation performance to another recent developed blind noise estimation approach.¹ Finally, we also evaluate the practical denoising performance of our noise estimation algorithm on medical images when it is used as a front-end to a denoiser that uses principal component analysis with local pixel grouping (LPG-PCA)² technique.

Keywords: Medical Imaging, Parallel Acquisition, Local Noise Estimation, Image Denoising

1. INTRODUCTION

Advanced medical imaging acquisition such as SENSE³ and fFBP⁴ have become emerging techniques for rapid acquisition of medical images, which improve the patient safety by the reduction of scanning time. Due to the spatially encoding during the rapid parallel acquisition process, the reconstructed SENSE images are typically corrupted by spatially varying noise, which challenges the traditional denoising methods⁵ based on statistical model. As the result, these denoising methods usually produce excessive blurring of image structures in low-noise regions and enhancement of noise-generated image gradients in high-noise regions. Similarly, for various data acquisition geometries, e.g., parallel-beam, fan-beam, and cone-beam, the process of rapid acquisition of projection data and the corresponding FBP algorithm leads to a significant nonuniform noise distribution⁶ in the reconstructed CT images.

2. PREVIOUS WORKS

Recently, techniques have been intensively studied to address the denoising problem for MR images with spatially varying noise due to parallel imaging (e.g., SENSE). One early effort⁷ uses anisotropic diffusion denoising based on noise distribution obtained from sensitivity maps of MR scanner, however, such detailed information may not be available in clinical situations. Another approach¹ is proposed to recover noise map from the wavelet coefficients at higher frequency scales. However, the process of zeroing high-contrast edges can not effectively remove all tissue boundaries from the noise map due to the spatially spread of the wavelet coefficients associated with these high-contrast edges. Meanwhile, part of the real noise can be detected as high-contrast edges and falsely removed from the noise map. Though the non-local means denoising method⁸ can remove noise of non-Gaussian distributions (e.g., Rician) that is more natural in the medical images, it provides very little information of the local noise strength in pixel level. Recently, a state-of-the-art unbiased method⁹ is proposed to estimate

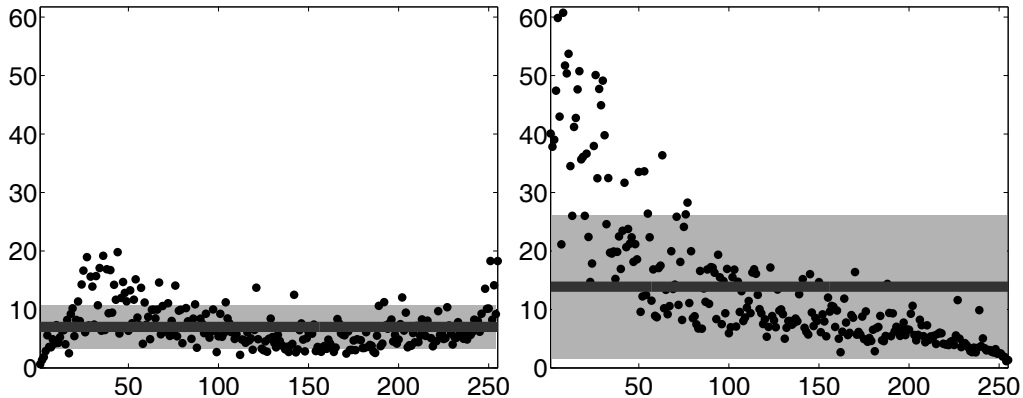


Figure 1. Kurtosis profiles of a clean medical image for two types of band-pass filtered domains: DCT (left) and FastICA (right), which demonstrate the kurtosis concentration phenomenon.

noise level in CT images. The proposed technique requires repeated CT scans of the object under examination, and thus may raise the risk of cancer as reported*.

In this work, we propose a novel method to estimate the local noise level in a single medical image without any prior knowledge of imaging device. Our method makes no assumption on the form of the underlying noise distribution and hence can be applied to reconstructed medical images with reconstruction noise of various distributions including Gaussian and Rician. We also report some preliminary experimental results by applying this method to estimate the noise of medical images and incorporating our method into a denoiser that uses the two-stage LPG-PCA method² to aid analysis of medical images.

3. METHOD

For a random variable x , the excess kurtosis κ that represents the peakedness of its probability distribution can be defined in terms of its variance σ and the fourth order central moment $\tilde{\mu}_4$ as $\kappa = \frac{\tilde{\mu}_4}{(\sigma^2)^2} - 3$. By this definition, a Gaussian variable has kurtosis zero, and natural images in the band-pass filtered domains have positive kurtosis values due to their super-Gaussian marginal statistics.¹⁰ Besides being positive, several recent works^{11, 12} have also pointed out that for natural images, kurtosis values across different band-pass filter channels present a concentration phenomenon, where the majority of the kurtosis values fall into a narrow range. As a special case of nature image, medical images also exhibit such statistical property.

Using a clean medical image and two different types of band-pass filter transforms, the kurtosis concentration phenomenon is demonstrated in Fig.1. The left subfigure is the kurtosis profile for using 255 band-pass filters from a 16×16 DCT decomposition in ascending order of their basic frequency, while the right subfigure is the one for adopting 255 band-pass filters obtained from the FastICA decomposition¹³ learned from overlapping patches of 16×16 pixels in size collected from the image. The dots are kurtosis values obtained from the responses of the image convolved with the band-pass filters corresponding to the order given in the horizontal axes. The solid line is the mean of these kurtosis values with the shaded region corresponding to plus/minus standard deviation. Except for a few outliers, most kurtosis values are found not far from their mean value, confirming the concentration behavior of the kurtosis values.

It has been widely observed that image kurtosis is closely related with image variance. Recently, an effective method¹² is presented to estimate the variance of noise added to a clean image at various stages of production. The method assumes the kurtosis of natural images is constant across different DCT bands. However, it has two major drawbacks. First, it can only estimate global noise level for an entire image, while we need detail local noise level information for post-processing of medical images. Furthermore, this method estimates noise level with an iterative numerical algorithm, which is typically not optimal.

*News source: <http://www.npr.org/templates/story/story.php?storyId=121436092>.

To address these two problems, we introduce a novel method to estimate local noise level in image, which can reach the optimum with a closed form solution. Let us denote a clean medical image \mathbf{x} , and $\mathbf{y} = \mathbf{x} + \mathbf{z}$ as a result of \mathbf{x} contaminated by a additive white Gaussian noise (AWGN) \mathbf{z} of unknown variance σ^2 . Our goal is to estimate σ^2 from \mathbf{y} . To this end, we produce the response image y_k by the convolution of y with the k th filter from the $N \times N$ DCT basis. We further denote κ_k , $\tilde{\kappa}_k$, and $\tilde{\sigma}_k^2$ as the kurtosis of x_k and y_k , and the variance of y_k , respectively. The kurtosis of x_k and y_k , and the variance of y_k and σ^2 are related as:¹⁴ $\tilde{\kappa}_k = \kappa_k \left(\frac{\tilde{\sigma}_k^2 - \sigma^2}{\tilde{\sigma}_k^2} \right)^2$. Assume the marginal distributions of band-pass filter responses, x_k has super-Gaussian property, i.e. $\kappa_k > 0$, we have $\tilde{\kappa}_k > 0$ due to the fact that $\tilde{\sigma}_k^2 > \sigma^2$. We can further take square root on the equation to obtain:

$$\sqrt{\tilde{\kappa}_k} = \sqrt{\kappa_k} \left(\frac{\tilde{\sigma}_k^2 - \sigma^2}{\tilde{\sigma}_k^2} \right). \quad (1)$$

Assuming that kurtosis values of medical image are approximately constant across different DCT bands, we can estimate the kurtosis of the medical image κ and its variance σ^2 by solving a nonlinear optimization problem:

$$L(\sqrt{\kappa}, \sigma^2) = \sum_{k=1}^{N^2} \left(\sqrt{\tilde{\kappa}_k} - \sqrt{\kappa} + \frac{\sqrt{\kappa}\sigma^2}{\tilde{\sigma}_k^2} \right)^2. \quad (2)$$

A particularly appealing property of our noise estimation method is that the optimal solution to minimize the object function in Eq.(2) can be transformed to a closed form as:

$$\sqrt{\kappa} = \frac{\langle \sqrt{\tilde{\kappa}_k} \rangle_k \langle \frac{1}{(\tilde{\sigma}_k^2)^2} \rangle_k - \langle \frac{\sqrt{\tilde{\kappa}_k}}{\tilde{\sigma}_k^2} \rangle_k \langle \frac{1}{\tilde{\sigma}_k^2} \rangle_k}{\langle \frac{1}{(\tilde{\sigma}_k^2)^2} \rangle_k - \langle \frac{1}{\tilde{\sigma}_k^2} \rangle_k^2}, \text{ and } \sigma^2 = \frac{1}{\langle \frac{1}{\tilde{\sigma}_k^2} \rangle_k} - \frac{1}{\sqrt{\kappa}} \frac{\langle \sqrt{\tilde{\kappa}_k} \rangle_k}{\langle \frac{1}{\tilde{\sigma}_k^2} \rangle_k}, \quad (3)$$

where we use $\langle \cdot \rangle_k$ as a shorthand notation for the average over different band-pass filters.

It should be noted that even though we assume AWGN, this is not as restricted as it seems, as very non-Gaussian independent noise in the pixel domain will mix in to be Gaussian noise in the filter domain due to the central limit theorem and noise independence.

The global noise level estimation method can be further extended for the estimation of locally varying noise levels in reconstructed medical images. Instead of straightforward implementation using sliding estimation windows, we propose a more efficient local noise estimation algorithm based on *integral image*.¹⁵ In particular, the integral image of an image \mathbf{x} , denoted as $\mathcal{I}(\mathbf{x})$, is an image of the same dimension as \mathbf{x} , but its value at index (i, j) is the sum of all pixel values of \mathbf{x} in the rectangular area of $[1, i] \times [1, j]$. The integral image can be efficiently constructed [†], and it can be used to compute the sum in any rectangular sub-region $[i, i+I] \times [j, j+J]$ with three addition/subtraction operations as $\mathcal{I}(\mathbf{x})_{i+I, j+J} - \mathcal{I}(\mathbf{x})_{i, j+J} - \mathcal{I}(\mathbf{x})_{i+I, j} + \mathcal{I}(\mathbf{x})_{i, j}$. This makes it particularly useful for computing the local spatial moments for overlapping rectangular regions. Specifically, we can use the integral image to compute the k^{th} order spatial statistics for a region $\Omega = [i, i+I] \times [j, j+J]$, as:

$$\mu_k(\mathbf{x}_\Omega) = \frac{1}{\Omega} \left[\mathcal{I}(\underbrace{\mathbf{x} \circ \dots \circ \mathbf{x}}_{k \text{ times}})_{i+I, j+J} - \mathcal{I}(\underbrace{\mathbf{x} \circ \dots \circ \mathbf{x}}_{k \text{ times}})_{i, j+J} - \mathcal{I}(\underbrace{\mathbf{x} \circ \dots \circ \mathbf{x}}_{k \text{ times}})_{i+I, j} + \mathcal{I}(\underbrace{\mathbf{x} \circ \dots \circ \mathbf{x}}_{k \text{ times}})_{i, j} \right] \quad (4)$$

Furthermore, based on the relation between variance and kurtosis and the moments, the local variance and kurtosis of a surrounding rectangular region Ω of each pixel location can be computed as:

$$\kappa(\mathbf{x}_\Omega) = \frac{\mu_4(\mathbf{x}_\Omega) - 4\mu_3(\mathbf{x}_\Omega)\mu_1(\mathbf{x}_\Omega) + 6\mu_2(\mathbf{x}_\Omega)\mu_1(\mathbf{x}_\Omega)^2 - 3\mu_1(\mathbf{x}_\Omega)^4}{(\sigma^2(\mathbf{x}_\Omega))^2} - 3, \text{ and } \sigma^2(\mathbf{x}_\Omega) = \mu_2(\mathbf{x}_\Omega) - (\mu_1(\mathbf{x}_\Omega))^2. \quad (5)$$

We can substitute the results of Eqs.(5) into Eqs.(3) to find the local noise level in the medical image.

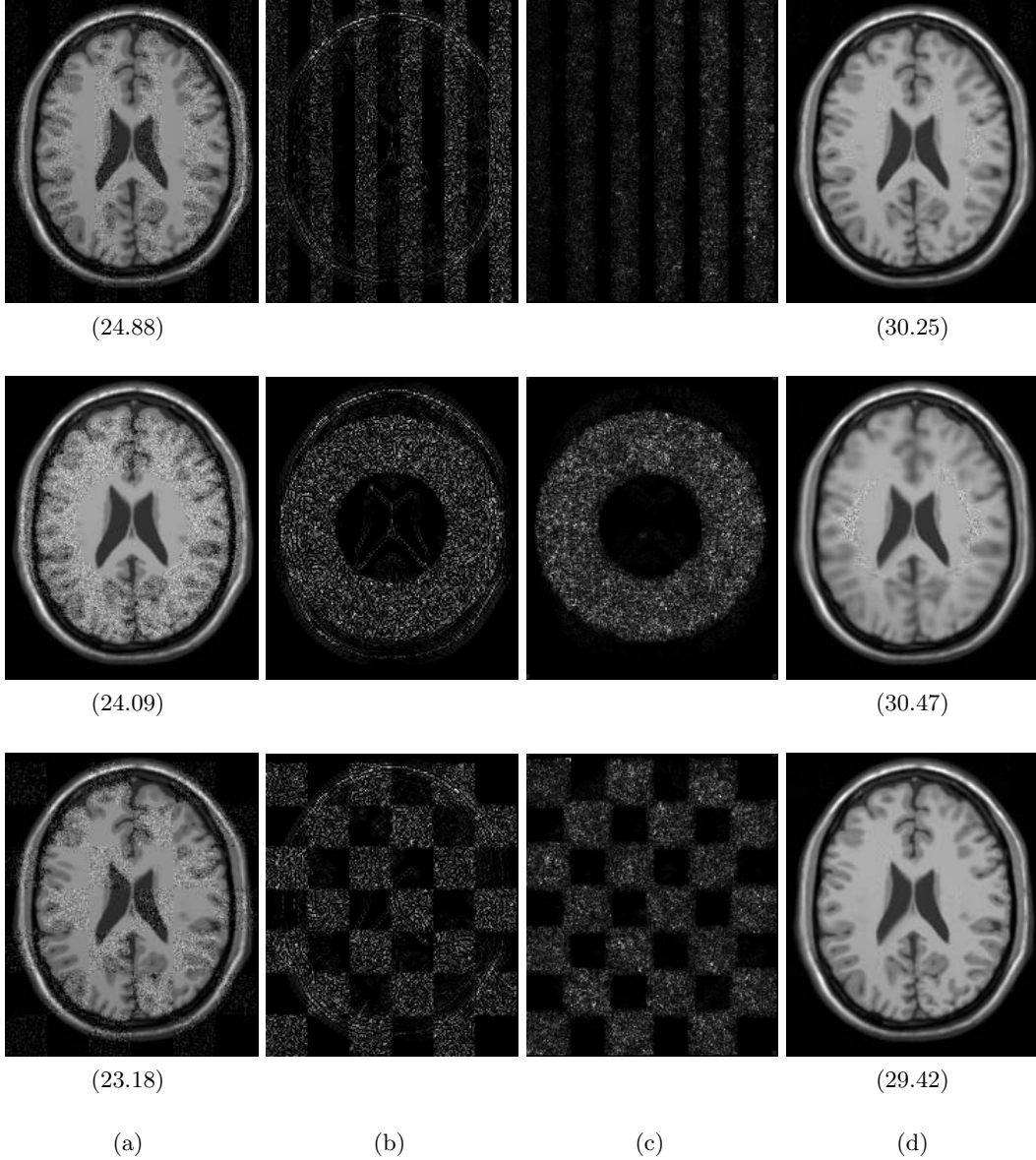


Figure 2. Comparison of local noise level estimation results. (a) MR brain images corrupted with noise of three different patterns. (b) Estimation results of the wavelet based method.¹ (c) Estimation results of our method. (d) The denoised MR brain images using the LPG-PCA method² with the local noise levels estimated by our method. In the parentheses are the PSNR values for corresponding noise corrupted and denoised brain images.

4. RESULTS

As a set of qualitative experiments, we first corrupt a MR brain image with spatially varying noise levels. As shown in the first column (a) of Fig.2, the top subfigure is a brain image corrupted with vertical stripes of AWGN of uniformly decreasing peak signal-to-noise ratio (PSNR) values, with PSNR = 25dB at the leftmost to PSNR = 20dB at the rightmost, where PSNR is the ratio between the maximum value of a signal and the strength of noise. The middle and bottom subfigures in (a) of Fig.2 are the images corrupted with AWGN of PSNR = 20dB with annulus and checkerboard patterns, respectively. The second and third columns (b and c) of Fig.2 are the local noise levels estimation results running Delakis's algorithm¹ and our method on these

[†]In MATLAB, it is implemented with two calls of function `cumsum`.

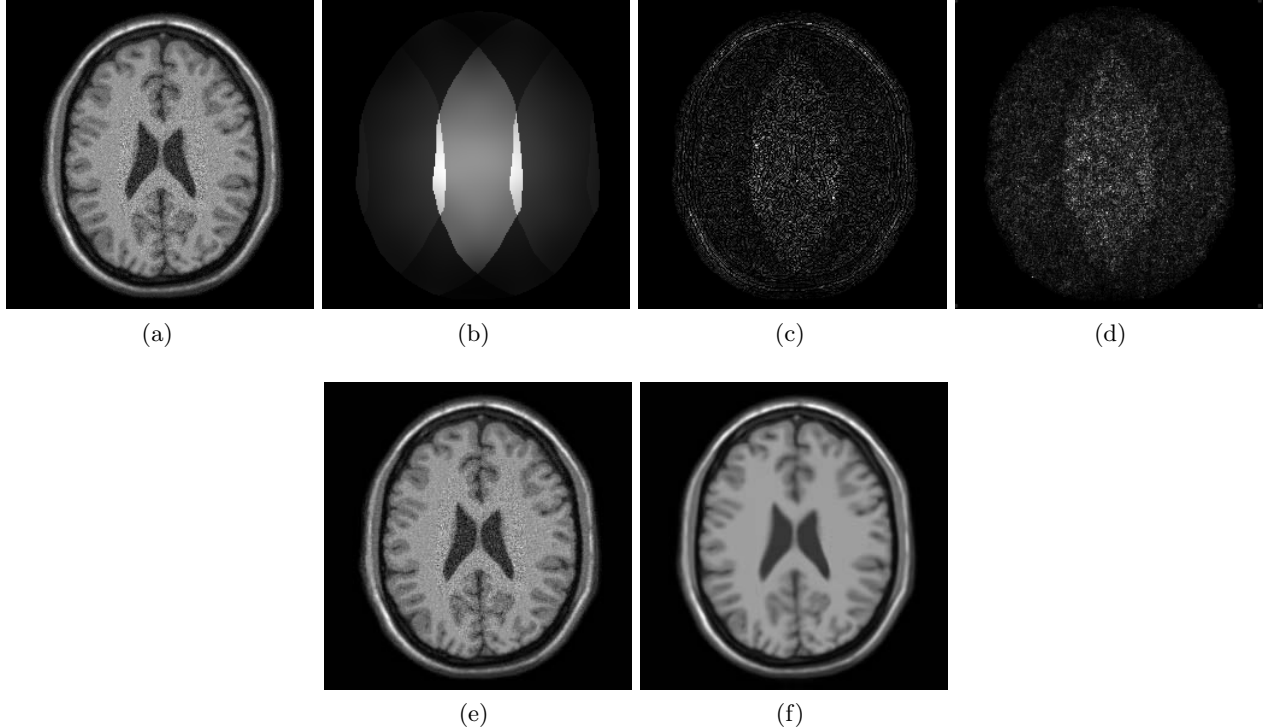


Figure 3. (a) A reconstructed SENSE image. (b) Noise map obtained using sensitivity matrix of MR scanner. Both images are courtesy of the original authors.⁷ (c) and (d) Local noise levels recovered by Delakis’s method¹ and ours, respectively. (e) and (f) Denoising results using LPG-PCA method² with single global noise level and with local varying noise levels estimated via our method, respectively.

images. Compared to Delakis’s algorithm, the local varying noise levels estimated using our method receive much less influence from high-contrast tissue boundaries, which pave the way for denoising that is quite necessary for medical image analysis. With the local varying noise levels estimated by our method using overlapping local blocks of 5×5 pixels in size, the MR brain images are denoised by the LPG-PCA method² that preserves the local image features after coefficient shrinkage in the PCA domain to reduce the noise. The denoising results are shown in the last column (d) of Fig.2, where the PSNR values of the denoised brain images increase for all three patterns compared to their noise corrupted counterparts in column (a).

We further apply our method to an actual SENSE image, which has spatially varying noise levels across the image due to the parallel acquisition process. Fig.3 (a) shows a SENSE image reconstructed from brain MR data, which has Rician noise with spatially varying levels caused by the three parallel scanning processes. The noise map of the SENSE image is obtained using the sensitivity matrix of MR scanner⁷ (b). The noise map calculated by the wavelet based method¹ is shown in (c). In comparison, the estimation using our method (d) appropriately recovers the spatial patterns of the varying noise levels with much less influence from tissue boundaries, which is consistent with the results in Fig.2. Fig.3 (e) and (f) show the denoised images of (a) using the LPG-PCA based method² with the single global noise level and with local varying noise levels estimated by our method. The denoising results demonstrate the advantage of using local varying noise levels instead of a global one when they are used as a preprocessing step for denoising before noise sensitive analyses are applied.

We finally evaluate quantitatively the performance of the proposed method on a set of computer-simulated MR brain images.¹⁶ In each image, we artificially add AWGN of various levels in a 100×100 pixels square region

	PSNR=25		PSNR=30		PSNR=35	
	w/ boundary	w/o boundary	w/ boundary	w/o boundary	w/ boundary	w/o boundary
Delakis Method ¹	47.02	46.89	25.60	25.33	14.88	15.03
Our Method	23.86	15.13	14.35	6.36	7.60	3.54

Table 1. Comparison of RMSE of the estimated noise level for Delakis’s method¹ and ours. The RMSEs are computed by both including and excluding the boundary pixels, where the boundary sizes are $\sqrt{|\text{ROI}|}/2$ (Delakis) and $\sqrt{|\Omega|}/2$ (Ours).

and further compute the root mean squared error (RMSE) between the estimated noise levels and the ground truth values in that region. Shown in table 1 is the performances comparison of our method ($\Omega = 30 \times 30$ pixels) with the work of Delakis (default setting),¹ which, to our best knowledge, is the only existing work that estimates local noise levels from a single MR image. Experimental results demonstrate that our method outperforms the wavelet based method in both high and low PSNR cases. Due to the variance of added noise, the noise level at each pixel location may not be exactly consistent with that of the entire 100×100 pixels square region. However, these set of experiments are able to compare the average local noise estimation performance of these two methods assuming the location of the noise region is known.

5. CONCLUSIONS

In this work, based on the kurtosis concentration property of medical images in band-pass filtered domains, we describe a method that estimates local noise levels in a single medical image without resorting to specific details of the imaging device. Experimental results show that our method can effectively estimate the local noise levels in SENSE MR images. We further evaluate the practical denoising performance of the proposed noise estimation algorithm on medical images by combining it with a LPG-PCA based denoiser. As a natural extension, we plan to apply this technique to CT images reconstructed with fFBR algorithm.

REFERENCES

- [1] Delakis, I., Hammad, O., and Kitney, R. I., “Wavelet-based de-noising algorithm for images acquired with parallel magnetic resonance imaging (MRI),” *Physics in Medicine and Biology* **52**, 3741–3751 (2007).
- [2] Zhang L., Dong W., Z. D. and G., S., “Two-stage image denoising by principal component analysis with local pixel grouping,” *Pattern Recognition* **43**, 1531–1549 (2010).
- [3] Pruessmann, K. P., Weiger, M., Scheidegger, M. B., and Boesiger, P., “SENSE: Sensitivity encoding for fast MRI,” *Magnetic Resonance in Medicine* **42**(5), 952–962 (1999).
- [4] Noo, F., Defrise, M., Clackdoyle, R., and Kudo, H., “Image reconstruction from fan-beam projections on less than a short scan,” *Physics in Medicine and Biology* **47**, 2525–2546 (2002).
- [5] Portilla, J., Strela, V., Wainwright, M. J., and Simoncelli, E. P., “Image denoising using scale mixtures of gaussians in the wavelet domain,” *IEEE Transactions on Image Processing* **12**(11), 1338–1351 (2003).
- [6] Zeng, G. L., “Nonuniform noise propagation by using the ramp filter in fan-beam computed tomography,” *IEEE Transactions on Medical Imaging* **23**(6), 690–695 (2004).
- [7] Samsonov, A. A. and Johnson, C. R., “Noise-adaptive nonlinear diffusion filtering of MR images with spatially varying noise levels,” *Magnetic Resonance in Medicine* **52**(4), 798–806 (2004).
- [8] Manjn, J. V., Coup, P., Mart-Bonmat, L., Collins, D. L., and Robles, M., “Adaptive non-local means denoising of MR images with spatially varying noise levels,” *J. Magn. Reson. Imaging* **31**(1), 192–203 (2010).
- [9] Wunderlich, A. and Noo, F., “Band-restricted estimation of noise variance in filtered backprojection reconstructions using repeated scans,” *IEEE Transactions on Medical Imaging* **29**(5), 1097–1113 (2010).
- [10] Burt, P. and Adelson, E., “The Laplacian pyramid as a compact image code,” *IEEE Transactions on Communication* **31**(4), 532–540 (1981).
- [11] Bethge, M., “Factorial coding of natural images: how effective are linear models in removing higher-order dependencies?,” *J. Opt. Soc. Am. A* **23**(6), 1253–1268 (2006).
- [12] Zoran, D. and Weiss, Y., “Scale invariance and noise in nature image,” *IEEE 12th International Conference on Computer Vision, ICCV 2009, Kyoto, Japan, September 27 - October 4, 2009* (2009).
- [13] Hyvärinen, A., “Fast and robust fixed-point algorithms for independent component analysis,” *IEEE Transactions on Neural Networks* **10**(3), 626–634 (1999).
- [14] Pauluzzi, D. R. and Beaulieu, N. C., “A comparison of snr estimation techniques for the AGWN channel,” *IEEE Transactions on Communications* **48**(10), 1681–1691 (2000).
- [15] Viola, P. and Jones, M., “Robust real-time object detection,” *International Journal of Computer Vision* **57**(2), 137–154 (2002).
- [16] Kwan, R. K., Evans, A. C., and Pike, G. B., “MRI simulation-based evaluation of image-processing and classification methods,” *IEEE Transactions on Medical Imaging* **18**(11), 1085–1097 (1999).